5-1999

The Arccos and Lommel Formulations—Approximate Closed-Form Diffraction Corrections

Charles J. Daly
Rochester Institute of Technology

Navalgund A. H. Rao
Rochester Institute of Technology

Recommended Citation
C. J. Daly and N. A. H. K. Rao, "The arccos and Lommel formulations—Approximate closed-form diffraction corrections," J. Acoust. Soc. Am. 105, 3067–3077 (1999) https://doi.org/10.1121/1.424636

The arccos and Lommel formulations—Approximate closed-form diffraction corrections

Charles J. Daly[a] and N. A. H. K Rao[b]
Chester F. Carlson Center for Imaging Science, Rochester Institute of Technology, Rochester, New York 14623

(Received 30 December 1997; accepted for publication 9 March 1999)

A closed-form frequency-domain formalism for spatially integrated diffraction corrections is proposed. Spatially integrated diffraction corrections are necessary when trying to characterize material with ultrasonic probing. In the case of piston transducers and point receivers, the Lommel diffraction formulation is used when the excitation is monochromatic, and the arccos diffraction formulation is used when the excitation is impulsive. The Lommel and arccos formulations are usually treated separately; here, they are connected. Specifically, the arccos diffraction formulation and Lommel diffraction formulation are shown to form an approximate Fourier transform pair. Since the Lommel formulation is amenable to closed-form spatial integration, Lommel functions are used to derive diffraction corrections for unfocused piston transducers operating in receive-only (one-way) mode or transmit/receive (two-way) mode. Results obtained from the proposed closed-form frequency-domain formalism are qualitatively compared with results based on the closed-form time-domain or impulse-response formalism. It will be shown that the proposed frequency-domain formalism has theoretical and practical value. Finally, specific computational considerations are discussed as necessary. © *1999 Acoustical Society of America.* [S0001-4966(99)03506-7]

PACS numbers: 43.20.Rz, 43.20.Fn, 43.20.Bi [DEC]

INTRODUCTION

Diffraction corrections are necessary when trying to characterize material, such as germanium or human tissue, with ultrasound.[1] They are also necessary when trying to predict or calibrate transducer responses.[2,3] Traditionally, the Lommel diffraction formulation[1,4] has been used when the excitation is monochromatic, and the arccos diffraction formulation[5,6] has been used when the excitation is a delta function. In this theoretical paper, the two formulations are connected, and Lommel functions are used to derive closed-form spatially integrated diffraction corrections for unfocused piston transducers operating in pulsed mode.

Piston transducers have been researched for over 50 years. Indeed, closed-form spatially integrated diffraction corrections have already been derived using both the arccos diffraction formulation[2,3,7] and the Lommel diffraction formulation.[8,9] This paper complements and extends the existing literature in three important ways. First, the arccos and Lommel diffraction formulations are compared, and the Fourier equivalence of the two is rigorously demonstrated. The term *Fourier equivalence* implies the two formulations form an approximate Fourier transform pair. Second, the theoretical development serves to review and unify the arccos and Lommel diffraction formulations for unfocused piston transducers. Papers on focused piston transducers are listed in Refs. 8, 10, and 11.

The third point requires detailed discussion. This paper proposes a closed-form frequency-domain formalism for spatially integrated one-way and two-way diffraction correction. The frequency-domain formalism is based on the Lommel diffraction formulation and, as such, serves as an alternative to the well-established time-domain or impulse response formalism based on the arccos diffraction formulation.[2,6] Thus, we are primarily interested in frequency-domain results, particularly for spatially integrated diffraction effects.

To establish the formalism, we assume delta function excitation of an infinitely baffled, unfocused piston transducer that has an infinite bandwidth or Dirac response.[2] To validate the proposed frequency-domain formalism, we inverse Fourier transform the frequency-domain results and obtain estimated impulse responses. These estimated responses are compared to responses obtained from the time-domain formalism. Our primary purpose in doing so is to establish the theoretical validity of the proposed formalism.

An immediate criticism, then, is that the proposed frequency-domain formalism will suffer from Gibb's phenomenon[12] because an infinite bandwidth can never be adequately sampled. The criticism is valid; however, we counter that real transducers are bandlimited. Thus, the frequency-domain formalism will be of interest and of value if it can be easily and accurately computed across some bandwidth of interest. We will show that it can.

Although we point out a few possible advantages of the frequency-domain formalism, it is not our intention to stimulate or engage in unproductive debate. Indeed, we acknowledge at the outset that the time-domain formalism is the gold standard in ultrasonic diffraction theory. This acknowledgment, however, should not preclude theoretical research into alternative formalisms.

The paper is organized as follows. Section I explains

[a]Electronic mail: cjd6905@rit.edu
[b]Electronic mail: narpci@rit.edu

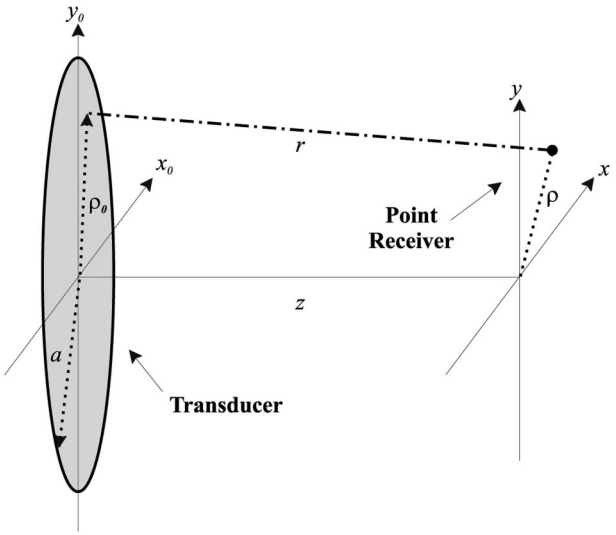

FIG. 1. Piston transducer and fictitious point receiver/scatterer.

more assumptions and defines terms and expressions. Section II demonstrates the Fourier equivalence of the arccos and Lommel diffraction formulations as an approximate Fourier transform pair. In Sec. III, closed-form spatially integrated diffraction corrections are derived. Specific computational considerations are discussed where appropriate. Detailed error analyses are not presented, and our results are compared with the existing literature in a qualitative fashion only.

I. PRELIMINARIES

Results from scalar diffraction theory will be applied to the diffraction problem depicted in Fig. 1. A pressure-sensitive piston transducer of radius a is shown. In the theoretical development, all transducers have a Dirac response and are assumed to be unfocused. The Kirchoff boundary conditions along with an infinite rigid baffle and spatially uniform excitation are assumed. For mathematical tractability, dispersion and multiple scattering are considered negligible. Attenuation is ignored, and only frequency-independent scattering is considered.

The transmitting transducer is symmetrically positioned at the origin of the $z=0$ plane. The position and dimensions of the pressure-sensitive receiver will be explicitly stated in the development. The velocity of the transducer disk, often denoted u_0, due to either monochromatic or impulsive excitation is assumed to be unity and does not appear in the development. The theory will be developed for unfocused transducers but should be easily extended to the focused case via the Lommel diffraction formulation for focused radiators developed by Papoulis (Ref. 13, pp. 351–353). Other assumptions will be explained as the need arises.

The term *one-way* implies that an ultrasonic transducer emits energy and another transducer coaxially located with the transmitter some distance z away acts as a receiver. The usual goal of one-way ultrasonic probing is to extract information about the medium between the transmitter and receiver. This information is encoded on the output voltage of the receiver. The output voltage is assumed to be proportional, in some manner, to the total pressure on the face of the receiver,[14,2,15] and the total pressure is found by spatially integrating the incoming pressure field over the receiving aperture. Note the receiving aperture is referred to as a *measurement circle* by Williams.[16] When properly formulated, this spatial integration gives a quantitative estimate of attenuation at different frequencies due to one-way diffraction.

The term *two-way* implies reflection imaging in which diffraction occurs during transmission and reflection. The notion of one-way and two-way is subject to quantitative interpretation. Specifically, some authors[1,2,8,17,18] state that equations derived for the one-way case can be used for the two-way case by simply doubling the depth z. This claim is based on an optical or mirror-image interpretation of reflection imaging and involves perfect reflection from an infinite plane. On the other hand, some authors[19–21] state that two-way diffraction can be characterized by an autoconvolution of the one-way impulse response. This claim is based on a linear systems or autoconvolution interpretation of reflection imaging. Only the mirror-image interpretation of reflection imaging is considered here. Discussion of spatially integrated autoconvolution diffraction corrections can be found in Refs. 22 and 23.

A number of mathematical expressions involving Bessel functions will be encountered in the derivations,[1,13,24] and they are defined here. Following Wolf,[24] u and v are real variables, n is a non-negative integer, and J_n denotes a Bessel function of the first kind of order n. U_n and V_n are Lommel functions defined by

$$U_n(u,v)=\sum_{s=0}^{\infty}(-1)^s\left(\frac{u}{v}\right)^{n+2s}J_{n+2s}(v), \tag{1}$$

$$V_n(u,v)=\sum_{s=0}^{\infty}(-1)^s\left(\frac{v}{u}\right)^{n+2s}J_{n+2s}(v). \tag{2}$$

Because they are infinite summations, the Lommel functions can be computed only approximately, and these approximations can be programmed either recursively[4,23] or explicitly in a do-loop. Do-loops were used in this work. W_n and Y_n denote the related functions

$$W_n(u,v)=\sum_{s=0}^{\infty}(-1)^s(s+1)\left(\frac{v}{u}\right)^{n+2s}J_{n+2s}(v), \tag{3}$$

$$Y_n(u,v)=\sum_{s=0}^{\infty}(-1)^s(n+2s)\left(\frac{v}{u}\right)^{n+2s}J_{n+2s}(v). \tag{4}$$

W_n are referred to here as Wolf functions, while Y_n are referred to as Hopkins functions.

Finally, since U_n converges too slowly for calculation when $u/v>1$, the following formulas from Gray and Mathews [Ref. 4, p. 185, Eq. (20)] will prove useful:

$$U_{2n+1}(u,v)+V_{-2n+1}(u,v)=(-1)^n\sin\left(\frac{1}{2}\left[u+\frac{v^2}{u}\right]\right), \tag{5a}$$

$$-U_{2n}(u,v)+V_{-2n}(u,v)=(-1)^n\cos\left(\frac{1}{2}\left[u+\frac{v^2}{u}\right]\right). \tag{5b}$$

Special case formulas for $u/v=1$ can be found in Gray and Mathews.

II. AN APPROXIMATE FOURIER TRANSFORM PAIR

In this section, derivations of the arccos and Lommel diffraction formulations are outlined, the two formulations are compared, and their equivalence as an approximate Fourier transform pair is rigorously demonstrated. The reader is referred to Oberhettinger,[5] Papoulis (Ref. 13, pp. 329–331), Stepanishen,[6] and Harris[24] for complete details on the derivations. The Lommel diffraction formulation is discussed first.

Assuming monochromatic excitation of the transducer in Fig. 1, the velocity potential sensed by a fictitious point receiver P located at some off-axis distance $\rho=\sqrt{x^2+y^2}$ can be written

$$H_1(\rho,z,\omega)=\frac{1}{2\pi}\int_{\sigma_o} f(\sigma_o)\frac{e^{-jkr}}{r}d\sigma_o, \tag{6}$$

where σ_o is the area of the transmitter. Throughout this paper, the subscript o denotes the $z=0$ plane, and the subscript 1 denotes one-way propagation. The velocity distribution across the face of the transducer is $f(\sigma_o)$ and is unity due to the assumption of spatially uniform excitation.

Equation (6) represents the Rayleigh-Sommerfeld diffraction integral for an infinitely baffled transducer.[6,25] It is important to note that Eq. (6) is based on Hyugen's principle and represents continuous integration of the free-space Green's function for a point source over a continuum of point sources which contains, mathematically speaking, an infinite number of point sources. As an aside, the velocity potential $H_1(\rho,z,\omega)$ is designated ψ_P in Ref. 1.

As usual, the time-dependence of $H_1(\rho,z,\omega)$ on $e^{j\omega t}$ is implied. The spatial wave number, k, is related to temporal frequency, ω, via $k=\omega/c$. Thus, the dependence of $H_1(\rho,z,\omega)$ on ω is implicit in two ways.

The Fresnel approximation,[13] in conjunction with circular symmetry, allows Eq. (6), to be estimated,

$$\begin{aligned} H_1(\rho,z,\omega)&\approx\hat{H}_1(\rho,z,\omega)\\ &=\frac{1}{z}e^{-jk(z+(\rho^2/2z))}\int_0^a e^{-jk(\rho_o^2/2z)}\\ &\quad\times J_0\left(\frac{k\rho}{z}\rho_o\right)\rho_o d\rho_o, \end{aligned} \tag{7}$$

where $\rho_o=\sqrt{x_o^2+y_o^2}$ is the off-axis distance at the $z=0$ plane and $\rho=\sqrt{x^2+y^2}$ is the off-axis distance at the z plane (Ref. 13, p. 330). The hat notation signifies estimation throughout this paper.

A prominent and familiar feature of Fresnel diffraction is its interpretation as a convolution involving a quadratic phase term.[13,26] This feature is obscured in Eq. (7). However, if the singularity function,

$$p_a(\rho_o)=\begin{cases}1, & \rho_o\leqslant a;\\ 0, & \rho_o>a,\end{cases} \tag{8}$$

is introduced in the integrand of Eq. (7) and the upper limit of integration changed to ∞, then Eq. (7) becomes

$$\begin{aligned} \hat{H}_1(\rho,z,\omega)&=\frac{1}{z}e^{-jk(z+\rho^{2/2z})}\int_0^\infty p_a(\rho_o)e^{-jk\rho_o^2/2z}\\ &\quad\times J_0\left(\frac{k\rho}{z}\rho_o\right)\rho_o d\rho_o \end{aligned} \tag{9}$$

which may be interpreted as the Hankel transform of the product of the singularity function $p_a(\rho_o)$ and a quadratic phase term. The convolution theorem for Hankel transforms allows Eq. (9) to be rewritten

$$\hat{H}_1(\rho,z,\omega)=\frac{1}{k}e^{-jk(z+\rho^2/2z)}\left[\frac{a}{\rho}J_1\left(\frac{ka\rho}{z}\right)*\frac{1}{j}e^{jk\rho^2/2z}\right], \tag{10}$$

where the convolution is with respect to $k\rho/z$. The familiar interpretation of Fresnel diffraction is made explicit in Eq. (10).

Equations (7) and (10) can be calculated numerically, but a closed-form expression would simplify the calculation. Equation (7) can be cast in closed form via Lommel functions. The closed-form result is

$$\begin{aligned} \hat{H}_1(\rho,z,\omega)&=\frac{1}{k}\exp\left[-j\left(kz+\frac{v^2}{2u}+\frac{u}{2}\right)\right]\\ &\quad\times[U_1(u,v)+jU_2(u,v)], \end{aligned} \tag{11}$$

where the substitutions $u=ka^2/z$ and $v=ka\rho/z$ result in more compact notation. Equation (11) is the Lommel diffraction formulation; it is easily programmed because of its closed form and is amenable to either direct or recursive calculation.

Seki *et al.*[1] used a variant of Eq. (11) to calculate pressure as a function of depth and off-axis distance; pressure can be obtained from Eq. (11) by multiplying by $j\omega\varrho$, where ϱ is medium density. Results obtained from Eq. (11) are plotted in Fig. 2. The plots agree well with those found in Seki's 1956 paper and serve to validate the use of Eq. (11) in the present work.

Three computational issues deserve mention here. First, Eq. (5) must be used when the ratio $u/v>1$. Specifically, U_n must be expressed in terms of V_n because U_n converges too slowly for calculation when $u/v>1$. Second, sufficient terms must be included in finite do-loop approximations to U_n. In our work, J_n up to and including $n=52$ have been used to calculate U_2. This high an order can be used if underflow is not too objectionable. Third, on-axis values of Eq. (11), that is when $\rho=0$, can be calculated via appropriate handling of the Lommel functions (Ref. 27, p. 540) when $v=0$, or they can be calculated from a separate formula which is easily derived by explicitly integrating Eq. (7) with $\rho=0$. The latter method was used in our computations.

In contrast to the Lommel diffraction formulation which can only be derived analytically, the arccos diffraction formulation can be derived either analytically[5] or geometrically.[6] A modified version of Oberhettinger's analytic derivation is outlined here because Oberhettinger's derivation points to the Fourier equivalence of the arccos and

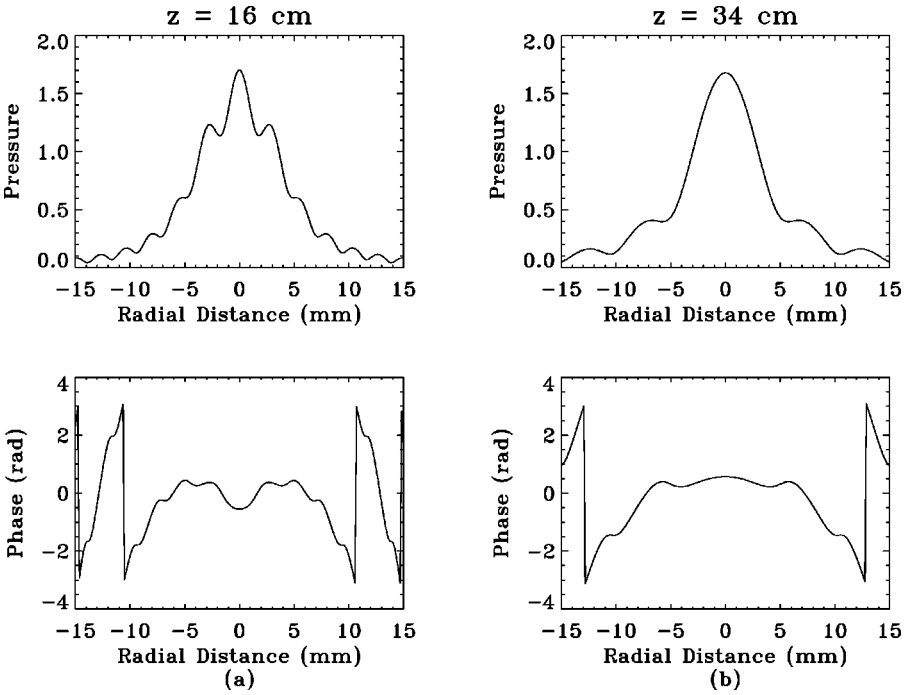

FIG. 2. Pressures after Seki *et al.*[1] via Eq. (11).

Lommel diffraction formulations; the modification involves application of the Fourier transform instead of the Laplace transform.

Assuming the transducer in Fig. 1 is excited by an impulse, the velocity potential sensed by a fictitious point receiver located at P can be written

$$h_1(\rho,z,t)=\frac{1}{2\pi}\int_{-\infty}^{\infty}H_1(\rho,z,\omega)e^{j\omega t}d\omega$$
$$=\mathcal{F}^{-1}\{H_1(\rho,z,\omega)\}, \tag{12}$$

where $\mathcal{F}^{-1}$ denotes the inverse Fourier transform. Thus, Eq. (12) is the inverse Fourier transform of $H_1(\rho,z,\omega)$ in Eq. (6). Note, $h_1(\rho,z,t)$ is designated $\Phi_D(t)$ in Oberhettinger's paper.[5]

With a transformation from rectangular to polar coordinates ($x=\rho\cos\phi$ and $y=\rho\sin\phi$), $H_1(\rho,z,\omega)$ in Eq. (6) becomes

$$H_1(\rho,z,\omega)=\int_{\phi_o=0}^{2\pi}\int_{\rho_o=0}^{a}\{[\rho^2+\rho_o^2-2\rho\rho_o$$
$$\times\cos(\phi-\phi_o)+z^2]^{-1/2}\exp[-jk(\rho^2+\rho_o^2$$
$$-2\rho\rho_o\cos(\phi-\phi_o)+z^2)]\}\rho_o d\rho_o d\phi_o. \tag{13}$$

After several steps, Oberhettinger obtains exact expressions for $h_1(\rho,z,t)$. For $\rho<a$,

$$h_1(\rho,z,t)=\begin{cases}0, & ct<z;\\ c, & z<ct<R';\\ \dfrac{c}{\pi}\arccos\left[\dfrac{(ct)^2-z^2+\rho^2-a^2}{2\rho((ct)^2-z^2)^{1/2}}\right], & R'<ct<R;\\ 0, & ct>R,\end{cases} \tag{14}$$

and, for $\rho>a$,

$$h_1(\rho,z,t)=\begin{cases}0, & ct<R';\\ \dfrac{c}{\pi}\arccos\left[\dfrac{(ct)^2-z^2+\rho^2-a^2}{2\rho((ct)^2-z^2)^{1/2}}\right], & R'<ct<R;\\ 0, & ct>R.\end{cases} \tag{15}$$

Taken together, Eqs. (14) and (15) represent the arccos diffraction formulation where $R'=\sqrt{z^2+(a-\rho)^2}$ and $R=\sqrt{z^2+(a+\rho)^2}$.

Note that Eq. (13), which is the Rayleigh-Sommerfeld integral for diffraction from a piston transducer, led to the arccos diffraction formulation. On the other hand, Eq. (7), which is the Fresnel approximation to Eq. (13), led to the Lommel diffraction formulation. Thus, we conclude that the arccos and Lommel diffraction formulations are closely related, and this relationship is explored more fully later in this section.

For now, we do well to describe the well-known behavior of the arccos diffraction formulation.[6] Figure 3, which will be discussed in detail later, can be used as a visual aid. For a fixed depth z, the on-axis velocity-potential impulse response $h_1(\rho,z,t)$ is a rectangular pulse starting at $t=z/c$; its amplitude is c. As ρ increases, the start time of the pulse remains $t=z/c$ but the trailing edge of the pulse moves closer to $t=z/c$. Simultaneously, the fall time of the trailing edge increases, and the trajectory of the fall is governed by the arccos term in Eq. (14). In short, the pulselike nature of the impulse response gradually decays with increasing ρ. For $\rho>a$, the impulse response no longer resembles a rectangular pulse, and its maximum value is something less than c. In addition, its start time is delayed in proportion to ρ.

For a fixed off-axis distance ρ, $h_1(\rho,z,t)$ has the same general shape at any depth z but is compressed in time as z

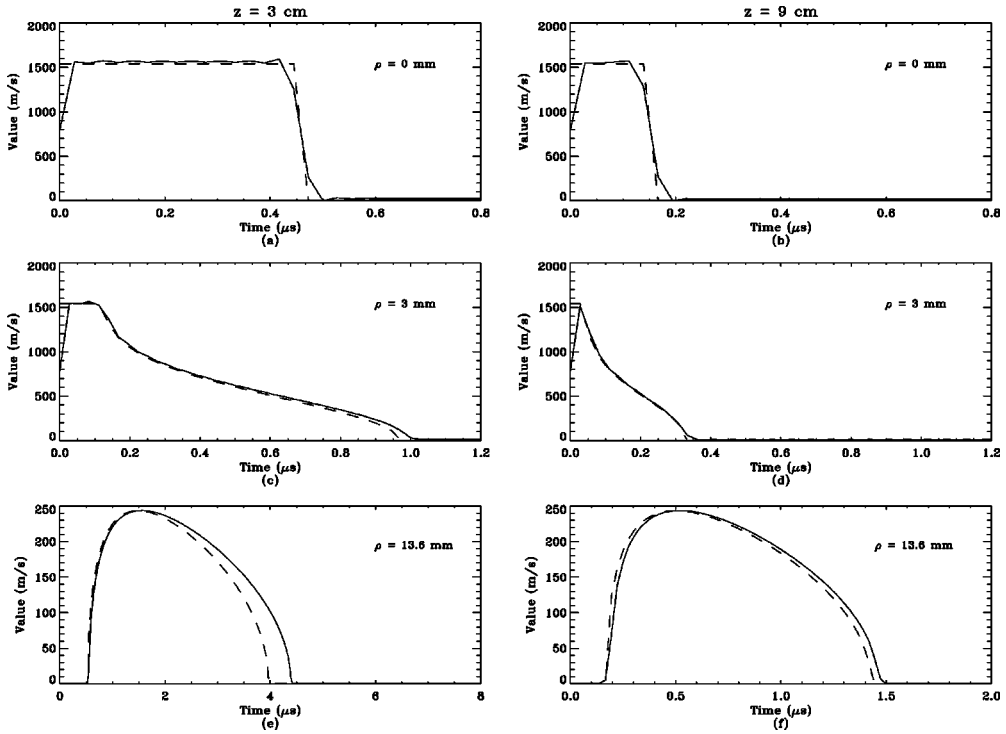

FIG. 3. One-way point-receiver impulse responses for the Lommel (solid) and arccos (dashed) diffraction formulations.

increases. The relationship can be quantified by expanding R' and R via binomial expansion, subtracting the smaller from the larger, and dividing for different values of z. The result is that for large z, $h_1(\rho,z,t)=h_1(\rho,z,z_r t/z)$, where z_r is some appropriately chosen reference plane.[2] Researchers in wavelet theory might find this an interesting physical problem since time scaling arises in a natural fashion.

As was just mentioned, the arccos and Lommel diffraction formulations are closely related. The Lommel diffraction formulation is a monochromatic frequency-domain solution based on the Fresnel approximation to the Rayleigh-Sommerfeld integral of scalar diffraction theory. Hence, the derivation of Lommel diffraction formulation permits monochromatic diffraction from a circular aperture to be interpreted as convolution involving a depth-dependent quadratic phase factor as in Eq. (10). On the other hand, the arccos diffraction formulation is a polychromatic time-domain solution based on the Rayleigh-Sommerfeld integral. The arccos formulation permits an interpretation of impulsive diffraction from a piston transducer in terms of a depth-dependent time-scaling operation.

The Fourier equivalence of the Lommel and arccos diffraction formulations will now be demonstrated. Consider again the general form of the arccos diffraction formulation, Eq. (12). In this equation, $h_1(\rho,z,t)$ is the inverse Fourier transform of some unspecified function, $H_1(\rho,z,\omega)$. Of course, $H_1(\rho,z,\omega)$ could be obtained by calculating $h_1(\rho,z,t)$ and Fourier transforming the result. Doing so, however, does not advance the goal of finding closed-form spatially integrated diffraction corrections.

Recall the Lommel diffraction formulation, $\hat{H}_1(\rho,z,\omega)$ in Eq. (11), is a closed-form estimate of $H_1(\rho,z,\omega)$ in Eq. (13). Further, the Lommel diffraction formulation is written in terms of $k=\omega/c$. Theoretically, discrete Fourier coefficients for the arccos diffraction formulation can be estimated using $\hat{H}_1(\rho,z,\omega)$. These coefficients can then be inverse Fourier transformed to obtain

$$\hat{h}_1(\rho,z,t)=\mathcal{F}^{-1}\{\hat{H}_1(\rho,z,\omega)\}, \tag{16}$$

which is, as already mentioned, an estimate of the impulse response predicted by the arccos diffraction formulation.

Thus, the Lommel diffraction formulation $\hat{H}_1(\rho,z,\omega)$ is a closed-form approximation of the Fourier transform of the arccos diffraction formulation $h_1(\rho,z,t)$, and Eq. (11) can be used to sample the arccos diffraction formulation in the frequency domain. In short, the Lommel and arccos diffraction formulations form an approximate Fourier transform pair,

$$\mathcal{F}\{h_1(\rho,z,t)\}\approx\hat{H}_1(\rho,z,\omega), \tag{17}$$

where $\mathcal{F}$ is the Fourier transform.

The Lommel diffraction formulation was used in conjunction with Eq. (16) to compute $\hat{h}_1(\rho,z,t)$, an estimate of $h_1(\rho,z,t)$, for three off-axis positions at two depths, $z=3$ and $z=9$ cm. The speed of sound was set at $c=1540$ m/s, and the diameter of the piston was set at $2a=13$ mm. We reiterate that the transducer was assumed to have an infinitely broadband or Dirac response, and the excitation was assumed to be an impulse. The sampling frequency was set at $f_S=36$ MHz; thus, the Nyquist frequency was 18 MHz. Note the sampling rate is consistent with 2X oversampling of a real 2.25-MHz piston transducer with a cutoff frequency of 4.5 MHz. More will be said about real transducers later.

The results are shown in Fig. 3. The off-axis positions are annotated in the figure. The impulse responses for a given ρ are plotted on the same time scale, referenced to t

$=z/c$, to emphasize the depth-dependent time scaling mentioned earlier. In all figures where the two diffraction formulations are compared, Lommel-derived results are plotted with solid lines, while arccos-derived results are plotted with dashed lines. In this work, the arccos diffraction formulation is the gold standard against which the Lommel diffraction formulation is compared.

Before analyzing the results, we discuss Gibb's phenomenon[12] and its impact on this work. Under the stated assumptions and for practical geometries, impulse responses computed using the arccos diffraction formulation have compact support in the time domain; consequently, their Fourier transforms have infinite bandwidth in the frequency domain. In practice, the Lommel diffraction formulation can be sampled only over some finite bandwidth (truncation in the frequency domain); consequently, impulse responses based on the Lommel diffraction formulation will suffer from Gibb's phenomenon.

As a result, we expect that Lommel-based results will fail to capture temporal discontinuities and will simultaneously exhibit ringing in the neighborhood of any temporal discontinuities. The degree of failure and extent of ringing are functions of the sampling rate; higher sampling rates will capture temporal discontinuities more faithfully but simultaneously introduce more ringing. In short, impulse responses based on the Lommel diffraction formulation and Eq. (16) can never show exact agreement with those based on the arccos diffraction formulation in Eqs. (14) and (15).

The plots in Fig. 3(a) and (b) show on-axis impulse responses. As was explained earlier, the on-axis impulse response for a piston transducer is a rectangular pulse of amplitude c that gets compressed in time with increasing depth z. The on-axis impulse responses computed with the Lommel diffraction formulation capture this behavior. As expected, they do not capture the discontinuities at the beginning and end of each pulse. Note that for $\rho=0$, the Fresnel approximation is very good. Thus, it can be argued that the disagreement at the discontinuities is due primarily to Gibb's phenomenon.

Figure 3(c) and (d) show impulse responses for $\rho=3$ mm. Here again, the disagreement, mostly near discontinuities, is due to Gibb's phenomenon and not due to the Fresnel approximation. The Lommel-based results are consistent with the results predicted by the arccos diffraction formulation.

The plots in Fig. 3(e) and (f) show impulse responses for $\rho=13.6$ mm. Since $\rho>a$, each impulse response will have a maximum amplitude less than c and will start at some time later than $t=z/c$. This behavior is confirmed in the plots. Note that the Lommel diffraction formulation overestimates the time duration of both impulse responses. Since ρ is large, the disagreement here is primarily due to the fact that the Lommel diffraction formulation is based on the Fresnel approximation.

Overall, the results show satisfactory agreement and confirm the validity of the Fourier equivalence of the arccos and Lommel diffraction formulations as an approximate Fourier transform pair. Clearly, the magnitude and phase responses computed using the Lommel diffraction formulation capture the salient features of the arccos diffraction formulation. Thus, no discussion or graphs of frequency-domain results are included at this point. We will discuss frequency-domain results in great detail in the next section.

The three computational issues already mentioned apply here, and five new ones require discussion. Because these issues will resurface, these issues will be referred to as the *five general computational issues*. First, the arccos impulse is real; hence, Fourier coefficients need be calculated for positive frequencies only. Negative-frequency coefficients are simply the complex conjugate of the positive-frequency coefficients.

This computational benefit is negated by the fact that the Lommel diffraction formulation is ill-defined at $\omega=0$. Thus, a DC frequency coefficient cannot be calculated directly. It can, however, be indirectly calculated by exploiting the positivity of the arccos diffraction formulation. In this work, discrete Fourier coefficients were calculated via Eq. (11) and inverse Fourier transformed with the fast Fourier transform (FFT). The resulting samples were forced to be greater than or equal to zero. In short, $\hat{h}_1(\rho,z,t)$ was forced to be positive. These two issues represent a trade-off inherent in any Lommel-based solution.

The k in the denominator of Eq. (11) is the third issue. Since the coefficients calculated from the Lommel formulation are ultimately sent to an FFT algorithm, continuous or discrete frequencies may be used with k. Discrete frequencies were used in our implementation. If the results are to be scaled to a maximum value of unity, the choice is immaterial.

Fourth, as explained earlier, estimated impulse responses will suffer from ringing due to Gibb's phenomenon due to truncation in the frequency domain. If desired, this artifact can be reduced with frequency-domain windowing; a window $w(f)=\mathrm{sinc}(0.25\pi f/f_S)$, where $\mathrm{sinc}(x)=\sin(\pi x)/(\pi x)$, was used to produce the results shown in Fig. 3. The window is admittedly *ad hoc*, but it produced satisfactory results.

Finally, Eq. (11) gives no indication of how many frequency samples are required in estimating the arccos impulse response. For a given off-axis position ρ and sampling frequency $f_s=1/\Delta t$, the minimum number of samples required can be computed via $(R-z)/(c\Delta t)$ or $(R-R')/(c\Delta t)$, whichever is appropriate. Further, when comparing the two formulations, accurate book-keeping in terms of sampling frequency, zero-padding, amplitude scaling, and phase is essential because results are being computed in conjugate domains.

Clearly, the Lommel diffraction formulation is more difficult to compute than the arccos diffraction formulation. Nonetheless, this section has formally connected the two formulations, and this connection is of historical and theoretical interest. Indeed, it appears to be of practical interest. For example, Chen *et al.* used the Lommel diffraction formulation in their 1994 paper on acoustic coupling to and from a flat plate.[8] Furthermore, the Lommel diffraction formulation may find application in numerical computation of complicated diffraction expressions[21,28] involving piston transducers and the free-space Green's function for a point source.

III. SPATIALLY INTEGRATED DIFFRACTION CORRECTION

Over 20 years ago, Huntington, *et al.*,[27] Williams,[16,18] Seki *et al.*,[1] Bass,[14] Rhyne,[3] and Rogers and Van Buren[9] researched closed-form spatially integrated diffraction corrections. Khimunin[28] and Benson and Kiyohara[31] reported numerical results. More recently, Cassereau *et al.*[2] and Chen *et al.*[8] have continued the work of the early researchers.

The researchers just mentioned derived or calculated one-way diffraction corrections and ultimately invoked the optical or mirror-image interpretation of ultrasound to extend the one-way corrections to the two-way case; we invoke the same interpretation here. The works of Rhyne, Cassereau *et al.*, and Rogers and Van Buren are particularly germane to this paper, and more will be said about them in this section.

Given that one-way diffraction has been researched so extensively, we must explain why we are revisiting the topic. First, we wish to establish that the Fourier equivalence of the arccos and Lommel diffraction formulations is valid for spatially integrated diffraction. Second, we will gain new insight into diffraction from a piston transducer and derive at least one new equation of academic, if not practical, interest. Finally, we will gain confidence that the Lommel diffraction formulation can be applied in the numerical computation of complicated diffraction expressions involving piston transducers.

Closed-form results will be derived for two cases: (i) a piston receiver with radius $b \leqslant a$ and (ii) a piston receiver with infinite radius. In both cases, the transmitter, a piston transducer with radius a, and the receiver are coaxially located and separated by a distance z. Spatially integrating the Lommel diffraction formulation [Eq. (11)] for the first case yields

$$\langle \hat{H}_1(z,\omega)\rangle_b = 2\pi \int_0^b \hat{H}_1(\rho,z,\omega)\rho d\rho, \tag{18}$$

where the symbol $\langle\rangle$ subscripted with b denotes spatial integration over a disk of radius b. Note the angular integration from 0 to 2π has been completed.

The integral in Eq. (18) can be solved for $b \leqslant a$ with Wolf functions. Specifically, expand the integrand in terms of the V_n Lommel functions [Eq. (5)] and integrate using Lemma 9 in Ref. 24. With $v_b = kab/z$ and $u = ka^2/z$, the result is

$$\langle \hat{H}_1(z,\omega)\rangle_b = -\frac{2\pi z}{k^2} e^{-jkz}\left\{ j\frac{v_b^2}{2u} + e^{-j((u/2)+(v_b^2/2u))} \times [2W_2(u,v_b) - jW_1(u,v_b) + jW_3(u,v_b)]\right\}, \tag{19}$$

which can be simplified via the Hopkins functions to

$$\langle \hat{H}_1(z,\omega)\rangle_b = -\frac{2\pi z}{k^2} e^{-jkz}\left\{ j\frac{v_b^2}{2u} + e^{-j((u/2)+(v_b^2/2u))} \times [Y_2(u,v_b) - jY_1(u,v_b)]\right\}. \tag{20}$$

Equation (20) is relatively new in the literature on diffraction from an unfocused piston transducer.[22,29] It is, however, a difficult expression to compute and, as a result, may be of academic interest only. Nonetheless, the Hopkins functions are highly convergent, and the computational burden of calculating them may be eased by recursion relations.[33]

Equation (20) is valid for $b \leqslant a$; however, only the case $b = a$ is investigated. Using relations developed by Wolf,[23,30] it can easily be shown that Eq. (20) reduces to

$$\langle \hat{H}_1(z,\omega)\rangle_a = -\frac{2\pi z}{k^2} e^{-j[kz+(u/2)]}\left\{ j\frac{u}{2} e^{j(u/2)} + e^{-j(u/2)} \times \left[\frac{u}{2}J_1(u) - j\frac{u}{2}J_0(u)\right]\right\}. \tag{21}$$

Unlike Eq. (20), Eq. (21) is relatively easy to compute. We remark here that Eq. (21) is, with the exception of a multiplicative constant, the same as the result derived by Rogers and Van Buren.[9] Thus, comparing Eq. (21) to their result will yield no new historical insight.

Instead, the validity of Eq. (21) was checked against the work done by Bass and Williams. The parameters used were the same as in Bass's 1958 article: $c = 1200$ m/s, $a = 1$ cm, and $f = 0.956$ MHz. The data were obtained from (a) Bass's 1958 equation [Ref. 14, Eq. (14)], (b) Williams' 1970 equation [Ref. 18, Eq. (6)], and (c) Eq. (21). Note Williams (Ref. 18, p. 286) corrected two typos in Bass's 1958 equation.

The squared-magnitude results in decibels (dB) are presented in Figs. 4 and 5. The graphs show the spatially integrated diffraction effects, due to monochromatic excitation, plotted as a function of $S = z\lambda/a^2$; two graphs of Eq. (21) are included for the purposes of comparison. The oscillatory behavior of Bass's result at low S is due to the small number of terms used in his equation. The overall results, however, show excellent agreement, and the plots confirm the well-established fact that attenuation due to diffraction increases with depth z. Thus, we have gained new academic perspective on classic research with the help of Eq. (21), which is a special case of Eq. (20).

We now extend the Fourier equivalence of the arccos and Lommel diffraction formulations to spatially integrated diffraction effects. Spatially integrating the velocity-potential transfer function $H_1(\rho,z,\omega)$ and subsequently inverse Fourier transforming the result yields

$$\langle h_1(z,t)\rangle_b = \mathcal{F}^{-1}\{\langle H_1(z,\omega)\rangle_b\}. \tag{22}$$

Now, we invoke the Fourier equivalence of the arccos and Lommel diffraction formulations and write

$$\langle \hat{h}_1(z,t)\rangle_b = \mathcal{F}^{-1}\{\langle \hat{H}_1(z,\omega)\rangle_b\}. \tag{23}$$

Hence, Eq. (20) can be used to estimate the spatially integrated impulse response associated with the arccos diffraction formulation.

Theoretically, substituting $k = \omega/c$ in Eq. (23) should allow one to estimate the Fourier coefficients of the spatially integrated arccos impulse response. These coefficients can then be inverse Fourier transformed to obtain an estimate of the spatially integrated arccos impulse response. This reason-

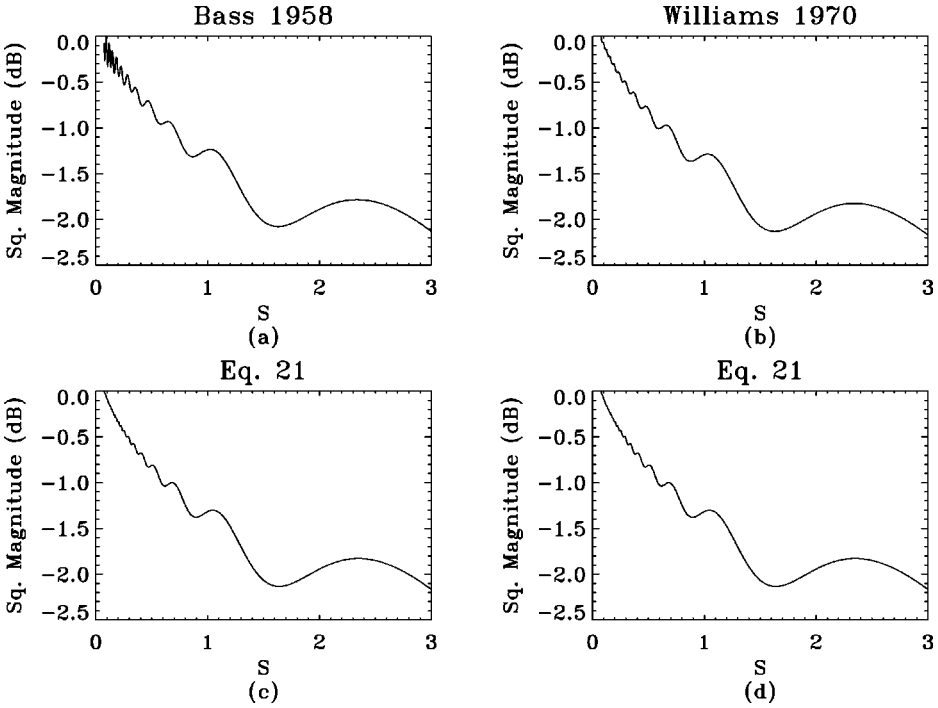

FIG. 4. Attenuation caused by diffraction as a function of S in both the near and far fields.

ing is simply an extension of the Fourier equivalence of the Lommel and arccos diffraction formulations developed for a point receiver in the previous section.

Some discussion is required before computing and comparing spatially integrated impulse responses. First, Rhyne[3] derived closed-form expressions for the spatially integrated arccos diffraction formulation for the case $b=a$; it serves as the gold standard in this work. As an important aside, Cassereau *et al.*[2] and, later, Daly and Rao,[7] generalized Rhyne's work; their closed-form expressions are completely general and include Rhyne's result as a special case.

Second, impulse responses computed using Rhyne's expressions have compact support in the time domain; consequently, their Fourier transforms have infinite bandwidth in the frequency domain. Like the Lommel diffraction formulation, Eq. (21) must be sampled over some finite bandwidth; consequently, impulse responses based on this equation will suffer from Gibb's phenomenon. Thus, the comments made earlier about impulse responses based on the Lommel diffraction formulation apply here. Those comments should be kept in mind when the comparison is made.

Figure 6(a) and (b) show spatially integrated one-way impulse responses estimated via Eq. (21) (solid lines) and spatially integrated one-way impulse responses calculated by using Rhyne's expression (dashed lines). The impulse responses were calculated for $b=a$ at two depths: $z=3$ and

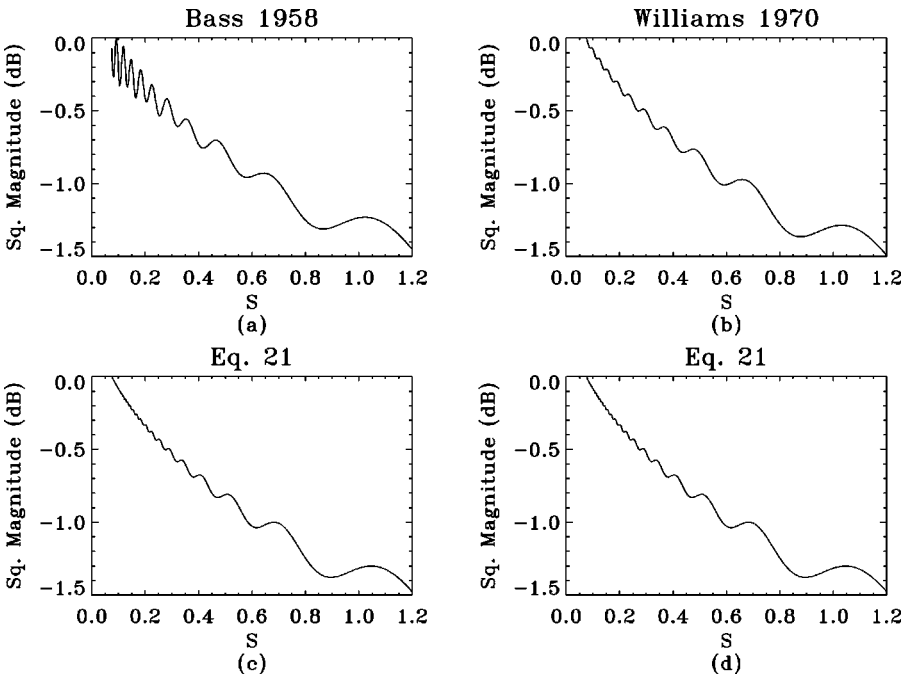

FIG. 5. Attenuation caused by diffraction as a function of S in the near field.

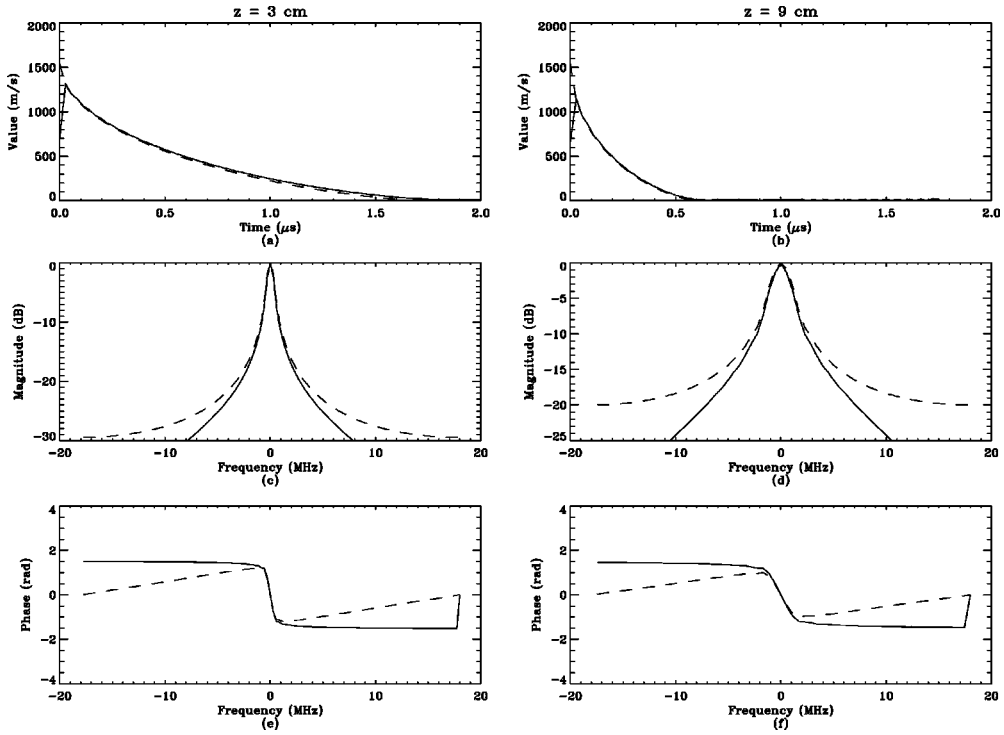

FIG. 6. Spatially integrated one-way impulse responses: Eq. (21) (solid) and Rhyne's expression (Ref. 3) (dashed).

$z=9$ cm. The speed of sound was set at $c=1540$ m/s, and the diameter of the piston was set at $2a=13$ mm. The transducer was assumed to have an infinitely broadband response, and the excitation was assumed to be an impulse. The sampling frequency was set at $f_S=36$ MHz; thus, the Nyquist frequency was 18 MHz.

With the exception of discontinuities, the impulse responses based on Eq. (21) are consistent with the results computed using Rhyne's expression and results computed by Kuc and Regula;[34] see Ref. 2 for an excellent discussion on the origin and effects of temporal discontinuities in spatially integrated impulse responses.

The five general computational issues mentioned in the previous section apply here. The window $w(f)$ discussed earlier was used in computing the Lommel-based impulse responses. Thus, ringing due to Gibb's phenomenon is reduced in the plots at the expense of a small amount of low-pass filtering. The impulse responses show satisfactory agreement. It is also important to reiterate how easy Eq. (21) is to compute. Furthermore, the utility of Eq. (21) is obvious if characterization of diffraction effects in the frequency domain is the main objective.

Figure 6(b) and (c) and Fig. 6(d) and (e) show the squared magnitude responses (dB) and the phase responses associated with the impulse responses in Fig. 6(a) and (b), respectively. Taking an optimistic point of view, we can say the magnitude responses show satisfactory agreement, particularly at the lower frequencies. Indeed, better agreement can be had at higher frequencies if the sampling frequency is increased, but the cost is more samples.

The phase responses do not agree as favorably. This is not surprising when one considers the physical origins of the results being compared. Specifically, the arccos-derived results are based on the Rayleigh-Sommerfeld diffraction integral, while the Lommel-derived results are based on the Fresnel diffraction integral. Hence, the two diffraction integrals differ primarily in terms of their phase.[26] This, in conjunction with Gibb's phenomenon, helps explain the phase differences exhibited in the plots.

It is crucial to note Eq. (21) was derived under the assumption of an ideal piston transducer with a Dirac response. Thus, Eq. (21) is completely general in terms of frequency. Real transducers, however, are bandlimited.

For example, consider a real 2.25 MHz unfocused piston transducer with diameter $2a=13$ mm. A typical bandwidth for such a transducer is 2 to 4 MHz centered at 2.25 MHz. Clearly, the results shown in Fig. 6 apply to the real transducer just described. Indeed, they apply quite well, particularly in terms of magnitude, with just 2X oversampling. Thus, if a diffraction correction were desired for this transducer, Eq. (21) could be used to calculate an inverse filter directly in the frequency domain. Furthermore, higher sampling rates could be used, and the results applied to real transducers operating at a higher frequency than 2.25 MHz.

Of course, the time-domain formalism developed by Rhyne[3] and extended by Cassereau *et al.*[2] could be used, and the impulse-response formalism is, in fact, more general. On the other hand, Eqs. (20) and (21) are amenable to calculation directly in the frequency domain across any bandwidth of interest, and Eq. (21) is very easy to compute. Clearly though, the time-domain formalism is easier to compute and more general than the Lommel-based equations. Nonetheless, we have demonstrated the validity of the proposed frequency-domain formalism for spatially integrated one-way diffraction.

More insight can be gained by considering the second

case: a piston receiver of infinite extent located some distance z from the transmitter. Consideration of this case leads to a theoretical result which further illustrates the utility of the proposed frequency-domain formalism. As an aside, this case can also be investigated in the time domain using the spatially integrated impulse formalism; the reader is referred to Ref. 2 for details.

Spatially integrating the Lommel diffraction formulation of Eq. (11) for this case yields

$$\langle \hat{H}_1(z,\omega)\rangle_\infty = 2\pi \int_0^\infty \hat{H}_1(\rho,z,\omega)\rho \; d\rho, \tag{24}$$

where the upper limit of infinity is not problematic because of the quickly converging Lommel functions in the integrand. With the help of Watson (Ref. 27, p. 541), Wheelon [Ref. 35, pp. 76–77, Eqs. (1.608) and (1.610)], and Euler's formula, it can be shown that

$$\langle \hat{H}_1(z,\omega)\rangle_\infty = -j\frac{\pi a^2}{k}e^{-jkz}. \tag{25}$$

This closed-form result is the same as the result reported by Williams in Ref. 18, Eq. (40) for monochromatic diffraction with a theoretically infinite receiver.

If Eq. (25) is used to calculate pressure, it yields the pressure, $\varrho\pi a^2 e^{-jkz}$, ''produced by a section of area πa^2 cut out of a plane wave that has the same particle velocity, [in our case unity], as does the piston source (Ref. 18, p. 289).'' In essence, the magnitude of the pressure detected by the infinite receiver is the same at all z-planes. No pressure/energy is lost because (i) the receiver is infinite and (ii) no loss mechanism has been introduced into the theory. Diffraction, in this case, introduces only a depth-dependent phase shift via the e^{-jkz} term.

Still more insight can be gained by examining Eqs. (21) and (25) more closely. Equation (21) can be rewritten,

$$\langle \hat{H}_1(z,\omega)\rangle_a = -j\frac{\pi a^2}{k}e^{-jkz} - \frac{\pi a^2}{k}e^{-jk[z+(a^2/z)]} \times\left[J_1\left(\frac{ka^2}{z}\right) - jJ_0\left(\frac{ka^2}{z}\right)\right]. \tag{26}$$

Note that the first terms of Eqs. (26) and (25) are identical. Thus, the second term in Eq. (26) represents combined diffraction/finite-receiver effects which serve to modify the infinite receiver solution of Eq. (25).[14,16] Equation (20) can be manipulated and interpreted in a similar fashion. At any rate, the $k=\omega/c$ in the denominator of the infinite receiver solution indicates that one-way diffraction is dominated by a $1/f$ low-pass filtering effect. This final insight further demonstrates the theoretical and practical value of the proposed frequency-domain formalism.

IV. CONCLUSION

Section II demonstrated the Fourier equivalence of the arccos and Lommel diffraction formulations as an approximate Fourier transform pair. In Sec. III, we used this equivalence to propose a new closed-form frequency-domain formalism describing spatially integrated diffraction effects from an unfocused piston transducer. The proposed frequency-domain formalism is based on the Lommel diffraction formulation and, in general, is in good agreement with results predicted by the time-domain or impulse-response formalism.

From a geometrical point of view, the time-domain formalism is superior to the proposed frequency-domain formalism because the former is based on the Rayleigh-Sommerfeld diffraction integral; thus, it is theoretically valid in the entire half-space in front of the transducer. On the other hand, the proposed frequency-domain formalism is strictly valid only in the Fresnel region. Nonetheless, the frequency-domain formalism has allowed us to compute a closed-form expression describing spatially integrated diffraction effects.

From a Fourier point of view, the Lommel-based formalism allows direct calculation of diffraction effects in the frequency domain (excluding DC) at whatever frequencies desired, and only positive coefficients need be calculated. Specifically, if a diffraction filter is to be used for inverse filtering or calibration of a real bandlimited transducer response, the filter can be readily calculated over the bandwidth of interest. If an impulse response is desired, the Lommel-based equations are problematic because they require a cumbersome estimation of DC and exhibit Gibb's phenomenon upon inverse Fourier transformation.

Computationally, the Lommel-based formalism is particularly easy to calculate for special case geometries ($b=a$) because no infinite summations are required. In general though, the time-domain formalism is easier to compute than the proposed frequency-domain formalism.

Ultimately, the time-domain formalism is superior to the proposed frequency-domain formalism in terms of geometrical validity and computational ease and efficiency. Nonetheless, the proposed frequency-domain formalism is of historical, theoretical, and practical interest. Indeed, we gleaned numerous insights from the proposed frequency-domain formalism and showed that it has potential application in diffraction correction (inverse filtering) of real bandlimited transducers. More details on the proposed frequency-domain formalism can be found in Refs. 23 and 32.

ACKNOWLEDGMENTS

The authors thank Emil Wolf, Wilson Professor of Optical Physics at the University of Rochester, New York, for his assistance. He discussed certain aspects of this work with Captain Daly, provided references, and pointed the way to others. The elegant results he derived in the 1950's made this paper possible. The authors also thank the reviewers for their insightful comments and helpful suggestions.

[1] H. Seki, A. Granato, and R. Truell, ''Diffraction effects in the ultrasonic field of a piston source and their importance in the accurate measurement of attenuation,'' J. Acoust. Soc. Am. **28**, 230–238 (1956).
[2] D. Cassereau, D. Guyomar, and M. Fink, ''Time deconvolution of diffraction effects–Application of calibration and prediction of transducer waveforms,'' J. Acoust. Soc. Am. **84**, 1073–1085 (1988).
[3] T. Rhyne, ''Radiation coupling of a disk to a plane and back or a disk to disk: An exact solution,'' J. Acoust. Soc. Am. **61**, 318–324 (1977).
[4] A. Gray and G. Mathews, *A Treatise on Bessel Functions and Their Ap-*

plications to Physics (Dover, New York, 1966). (First published in 1922.)
[5] F. Oberhettinger, ''On transient solutions of the ''baffled piston'' problem,'' J. Res. Natl. Bur. Stand., Sect. B **65**, 1–5 (1961).
[6] P. Stepanishen, ''Transient radiation from pistons in an infinite planar baffle,'' J. Acoust. Soc. Am. **49**, 1627–1638 (1971).
[7] C. Daly and N. Rao, ''Spatially averaged impulse response for an unfocused piston transducer,'' J. Acoust. Soc. Am. **105**, 1563–1566 (1999).
[8] X. Chen, K. Schwarz, and K. Parker, ''Acoustic coupling from a focused transducer to a flat plate and back to the transducer,'' J. Acoust. Soc. Am. **95**, 3049–3054 (1994).
[9] P. Rogers and A. Van Buren, ''An exact expression for the Lommel diffraction correction integral,'' J. Acoust. Soc. Am. **55**, 728–728 (1974).
[10] M. Fink and J. Cardoso, ''Diffraction effects in pulse-echo measurement,'' IEEE Trans. Sonics Ultrason. **SU-31**, 313–329 (1984).
[11] A. Penttinen and M. Luukkala, ''The impulse response and pressure nearfield of a curved ultrasonic radiator,'' J. Phys. D **9**, 1547–1557 (1976).
[12] R. Ziemer, W. Tranter, and D. Fanin, *Signals and Systems* (Macmillan, New York, 1983).
[13] A. Papoulis, *Systems and Transforms with Applications in Optics* (McGraw-Hill, New York, 1968), Chaps. 5 and 9.
[14] R. Bass, ''Diffraction effects in the ultrasonic field of a piston source,'' J. Acoust. Soc. Am. **30**, 602–605 (1958).
[15] G. Harris, ''Transient field of a baffled planar piston transducer having an arbitrary vibration amplitude distribution,'' J. Acoust. Soc. Am. **70**, 186–204 (1981).
[16] A. Williams, Jr., ''The piston source at high frequencies,'' J. Acoust. Soc. Am. **23**, 1–6 (1951).
[17] G. Kino, *Acoustic Waves: Devices, Imaging, & Analog Signal Processing* (Prentice-Hall, Englewood Cliffs, NJ, 1987).
[18] A. Williams, Jr., ''Integrated signal on circular piston receiver centered in a piston beam,'' J. Acoust. Soc. Am. **48**, 285–289 (1970).
[19] M. Fink, ''Theoretical study of pulsed echographic focusing procedures,'' in *Acoustical Imaging*, edited by P. Alais and A. Metherell (Plenum, New York, 1982), Vol. 10.
[20] J. Hunt, M. Arditi, and F. Foster, ''Ultrasound transducers for pulse-echo medical imaging,'' IEEE Trans. Biomed. Eng. **BME-30**, 453–481 (1983).
[21] J. Weight and A. Hayman, ''Observations of the propagation of very short ultrasonic pulses and their reflection by small targets,'' J. Acoust. Soc. Am. **63**, 396–404 (1978).
[22] J. Cardoso and M. Fink, ''Echographic diffraction filters and the diffraction function for random media through an instantaneous time-frequency approach,'' J. Acoust. Soc. Am. **90**, 1074–1084 (1991).
[23] C. Daly, ''The Arccos and Lommel Diffraction Formulations,'' Ph.D. thesis, Rochester Institute of Technology, 1998.
[24] E. Wolf, ''Light distribution near focus in an error-free diffraction image,'' Proc. R. Soc. London, Ser. A **204**, 533–548 (1951).
[25] G. Harris, ''Review of transient field theory for a baffled planar piston,'' J. Acoust. Soc. Am. **70**, 10–19 (1981).
[26] J. Gaskill, *Linear Systems, Fourier Transforms, and Optics* (Wiley, New York, 1978).
[27] G. Watson, *A Treatise on The Theory of Bessel Functions* (Cambridge University Press, New York, 1980). (First published in 1922.)
[28] E. Madsen, M. Insana, and J. Zagzebski, ''Method of data reduction for accurate determination of acoustic backscatter coefficient,'' J. Acoust. Soc. Am. **76**, 913–923 (1984).
[29] H. Huntington, A. Emslie, and V. Hughes, ''Ultrasonic delay lines. I,'' J. Franklin Inst. **245**, 16–23 (1948).
[30] A. Khimunin, ''Numerical calculation of the diffraction corrections for the precise measurement of ultrasound absorption,'' Acustica **27**, 173–181 (1972).
[31] G. Benson and O. Kiyohara, ''Tabulation of some integral functions describing diffraction effects in the ultrasonic field of a circular piston source,'' J. Acoust. Soc. Am. **55**, 184–184 (1974).
[32] C. Daly and N. Rao, ''Time- and frequency-domain descriptions of spatially averaged one-way diffraction for an unfocused piston transducer,'' Ultrasonics **37**, 209–221 (1999).
[33] E. Wolf, ''The X_n and Y_n functions of Hopkins, occurring in the theory of diffraction,'' J. Opt. Soc. Am. **43**, 218 (1953).
[34] R. Kuc and D. Regula, ''Diffraction effects in reflected ultrasound spectral estimates,'' IEEE Trans. Biomed. Eng. **BME-31**, 537–545 (1984).
[35] A. Wheelon, *Tables of Summable Series and Integrals Involving Bessel Functions* (Holden-Day, San Francisco, 1968).